Research Article Vol. 35, No. 7 / July 2018 / Journal of the Optical Society of America B 1557

Journal of the Optical Society of America B

OPTICAL PHYSICS

Vapor-cell frequency reference for short-wavelength transitions in neutral calcium

JENNIFER TAYLOR, BRYAN HEMINGWAY, JAMES HANSSEN, THOMAS B. SWANSON, AND STEVEN PEIL*

Time Service Department, United States Naval Observatory, 3450 Massachusetts Avenue, N.W., Washington, DC 20392, USA
**Corresponding author: steven.peil@navy.mil*

Received 28 February 2018; revised 3 May 2018; accepted 17 May 2018; posted 18 May 2018 (Doc. ID 325084); published 11 June 2018

We have characterized the molecular tellurium (Te_2) spectrum in the vicinity of the 423 nm $^1S_0$–$^1P_1$ and 431 nm $^3P_1$–$^3P_0$ transitions in neutral calcium. These transitions are relevant to optical clocks for atomic-beam characterization and cooling (423 nm) and enhanced detection (431 nm). The use of a Te_2 vapor cell as a frequency reference has many advantages over other laser stabilization techniques, and we discuss an application to measure the instability due to the second-order Doppler shift in a calcium beam clock.

OCIS codes: (140.3425) Laser stabilization; (120.6200) Spectrometers and spectroscopic instrumentation; (120.3930) Metrological instrumentation; (300.6390) Spectroscopy, molecular; (300.6210) Spectroscopy, atomic.

https://doi.org/10.1364/JOSAB.35.001557

1. INTRODUCTION

A. Operational Optical Clocks

Optical atomic clocks have resulted in dramatically improved performance over their microwave predecessors since their introduction in the past decade [1]. While state-of-the-art ion-trap and optical-lattice clocks provide the highest accuracy [2–4], there have been quite a few efforts in recent years to develop more robust, even portable, optical clock technology. These "operational" optical clocks could address applications that do not necessarily require absolute frequencies but could benefit from greater availability. Examples include operational clocks used for the generation of precise time [5,6], space clocks for applications such as global navigation [7], and field clocks for relativistic geodesy [8].

Although there has been some effort to engineer optical-lattice systems [9,10], in many cases the approach to building robust optical clocks has been to carry out spectroscopy on an atomic beam [11–13]. This is because laser technology is arguably the most serious obstacle to robust, continuous operation for an atomic clock (or any other atomic sensor). Aside from a frequency comb, a thermal (uncooled) beam clock can be constructed with a single laser for interrogation of the clock transition, although a second laser to enhance detection can dramatically improve performance. In comparison, an optical-lattice system requires a clock laser, a laser for creating the lattice, two lasers for cooling, and up to two lasers for re-pumping.

1. Atomic Beam Optical Clock

Optical clocks use alkaline-earth atoms or other elements with the same $^1S_0$ ground-state electronic structure, but only a subset of these elements are practical for atomic-beam clocks. The time available to excite a clock transition in a beam is short compared with the interaction time available in a trapped-atom system. For saturated absorption spectroscopy, measurement-time-limited resonances of the order of 500 kHz are typical [11,12], whereas a Ramsey–Bordé interrogation can generate linewidths from 50 kHz to below 5 kHz [12,13]. Therefore, the extremely narrow (typically 1 Hz or less), doubly forbidden $^1S_0$–$^3P_0$ transitions cannot be fully utilized in a beam clock; in fact, these weak transitions are difficult to excite in the short interaction time available, typically requiring laser power of order 1 W. The singly forbidden $^1S_0$–$^3P_1$ transitions are therefore better suited. In many $^1S_0$ ground-state atoms, the singly forbidden $^1S_0$–$^3P_1$ transition is relatively broad, and only a few elements have transitions with spectral widths that are fairly well matched with the interaction times one can achieve in a beam. These include strontium, calcium, and magnesium with $^1S_0$–$^3P_1$ transitions that have natural widths of 7 kHz, 375 Hz, and 40 Hz, respectively.

2. Calcium

Of the transitions mentioned above, the 657 nm $^1S_0$–$^3P_1$ transition in calcium (^{40}Ca) has some beneficial features. The 375 Hz width is narrow enough to not limit the resolution for even the best Ramsey–Bordé measurements, and the laser wavelength required for the strong $^1S_0$–$^1P_1$ transition used for cooling and other applications is much more convenient than for magnesium. In fact, calcium would be especially well suited for a cooled-beam clock, where resolutions approaching the natural width of the transition are achievable with the additional complexity of only one laser. Calcium was the subject

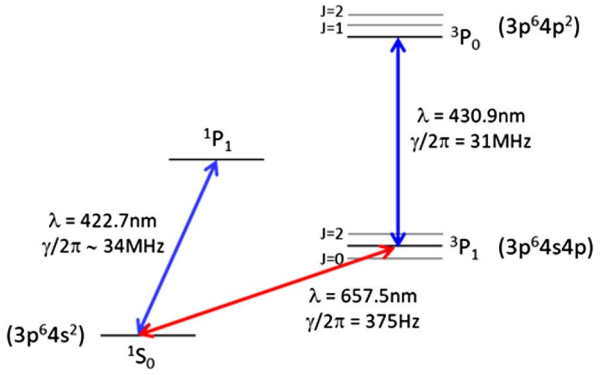

Fig. 1. Partial energy-level diagram for calcium (^{40}Ca), showing the clock transition at 657 nm and the blue transitions at 423 nm and 431 nm. Atoms in the $^3P_1$ excited clock state can be driven to a higher energy $^3P_0$ state with 431 nm light. Atoms in that state can only decay back to $^3P_1$ due to angular momentum selection rules, making the 431 nm transition a cycling transition useful for enhancing the detection signal.

of early precision optical spectroscopy [14,15] and subsequent cooled-atom optical clock efforts [16,17], but it was determined not to be ideally suited as a primary frequency standard. Yet, for the reasons presented, it has been the subject of recent efforts to build robust optical frequency standards that emphasize stability over accuracy.

One challenge with optical clocks based on calcium, or other $^1S_0$ ground-state atoms, is the availability of frequency references for stabilizing lasers tuned to the necessary optical transitions. While the interrogation laser is locked to the clock transition, lasers for other transitions need some other reference. In optical-clock atoms, there is typically a strong $^1S_0$–$^1P_1$ transition with a wavelength in the blue part of the spectrum. In calcium, this transition occurs at 422.792 nm, with a natural width of about 35 MHz; an energy level diagram is shown in Fig. 1. This line can be used for cooling [16,17], detection [12], or characterization of the oven and beam [18]. The $^3P_1$–$^3P_0$ transition in calcium at 431 nm, shown in the figure, is even better to use for detection; it can be driven to force an atom excited by the clock laser to scatter many blue photons, whereas the majority of the atoms remaining in the ground state do not contribute a background signal.

3. Laser Frequency Stabilization

Simple vapor cells are ideal for stabilizing the frequencies of lasers that are subsequently used for spectroscopy, cooling, or trapping, especially for applications that require long-term frequency stability or immunity to vibrations. They are routinely used for alkali-atom systems where the cells contain a vapor of the same element that is being used in the main apparatus. However, vapor cells are not an option for calcium or other $^1S_0$ ground-state atoms; at the necessary temperatures (of the order of 500°C) to create a reasonable vapor pressure for spectroscopy, calcium interacts with most glasses, rendering the glass opaque and the cell useless. These laser frequencies for calcium have typically been stabilized using a Fabry–Perot cavity or the atomic beam itself, but there are drawbacks of both of these techniques. A good cavity requires a high-vacuum chamber and thorough vibration isolation, especially if it is to be used during transport, and it will exhibit frequency drift at some level over long times. Locking to the atomic beam has the drawback of introducing additional vacuum windows and laser light to the clock vacuum chamber. Also, there are additional challenges to using the atomic beam to stabilize a laser to be used for the 431 nm detection line, since that signal relies on two resonant excitations. Less common frequency references that have been utilized for these wavelengths include heat pipes [19], vacuum vessels in which the spectroscopy windows are positioned away from a high-vapor region and held at a lower temperature, and hollow-cathode lamps [20]. Heat pipes are somewhat elaborate, requiring fabrication of a custom vacuum chamber, and hollow-cathode lamps can suffer from poorly understood frequency shifts and are known to be susceptible to plasma instabilities [21].

2. TELLURIUM VAPOR-CELL REFERENCE

A. Introduction

Molecular vapor cells have an abundance of transitions available to serve as frequency references because of the many rotational and vibrational modes. While molecular iodine has been a workhorse for frequency calibration and stabilization at wavelengths over much of the visible spectrum, its dissociation limit near 500 nm precludes its use at blue wavelengths. Like iodine, the tellurium dimer (Te_2) has many transitions due to molecular excitations, but tellurium can serve as a frequency reference well into the violet [22]. A sufficient vapor pressure for spectroscopy can be generated by heating tellurium to around 500°C, and it can be done using a standard glass cell since there are no deleterious reactions as in the case of calcium. Tellurium has been investigated generally [23] and used as a frequency reference for work on ytterbium [24] and barium ions [25], and for re-pumping in neutral strontium [26].

1. Experimental Setup

We investigate the tellurium spectrum using (saturated) absorption and modulation transfer spectroscopy (MTS) in a heated vapor cell while simultaneously driving the calcium transitions of interest. Light from a Ti:sapphire laser is passed through a commercial frequency-doubling cavity with a BBO (barium borate) crystal. For 2 W of near-IR light, we generate as much as 0.5 W of blue light. The frequency tuning of the Ti:sapphire laser required to reach both the calcium transitions of interest is accomplished using a birefringent filter. The doubling cavity has a modest bandwidth of about 1 nm for a fixed crystal orientation; re-orienting the BBO crystal allows the doubler to be tuned between the two wavelengths of interest, 8 nm apart, although with reduced efficiency. The blue light generated is fiber-coupled, sent through a fiber splitter, and sent to both a tellurium spectroscopy setup and a calcium atomic beam, as shown in Fig. 2.

Two different arrangements are used to look at the calcium response. For the 423 nm $^1S_0$–$^1P_1$ transition, shown in Fig. 2(b), we send several mW of laser light transverse to the atomic beam and measure the transmitted power. This gives an absorption resonance at the true calcium frequency, without any Doppler shift. The laser light in this path can have known

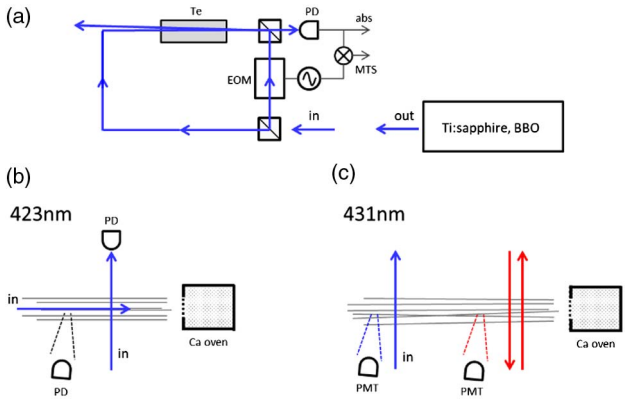

Fig. 2. Illustration of the setup used to measure the Te_2 spectrum in the vicinity of the corresponding calcium transitions. (a) Illustration of the absorption and MTS setup to measure Te_2 spectrum. Bottom: arrangement of laser beams used to measure (b) the 423 nm resonance and (c) the 431 nm resonance in a calcium beam. The laser transverse to the atomic beam in (b) can have known frequency shifts introduced for calibration. Thick (blue/red) lines with arrowheads represent laser light. The thin black lines in (a) represent electronic signals. PD, photodiode; PMT, photomultiplier tube; abs, absorption signal output; MTS, modulation transfer spectroscopy output.

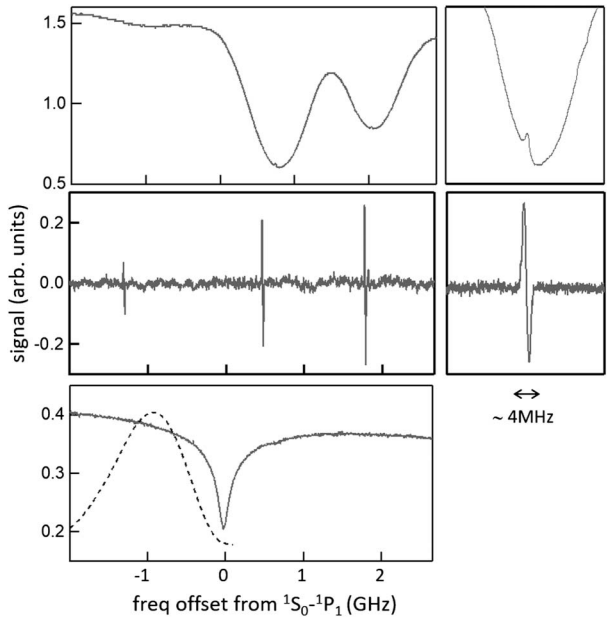

Fig. 3. Tellurium and calcium resonances near 422.79 nm. Left: three tellurium lines in the vicinity of the calcium $^1S_0$ – $^1P_1$ transition are shown via absorption curves (top) and demodulated MTS signals (middle). The calcium resonances for absorption of laser light transverse to the atomic beam direction (solid line), and the fluorescence from light propagating against the trajectory of the atoms (dashed line) are shown in the bottom plot. The fluorescence curve is scaled to fit on the plot. The slope on the background of the absorption curve reflects a slight frequency dependence in the doubler output. Barely visible are saturated absorption dips in the absorption resonances in the top plot and a signal from calcium-44 in the shoulder of the calcium absorption curve. Right: a closer look at some of the features in the plots on the left by scanning over a smaller range of frequencies.

frequency shifts introduced using an acousto-optic modulator for calibration. Simultaneously, we send several mW of light counter-propagating to the atomic beam and collect fluorescence from the atoms. This resonance is shifted due to the average velocity of the beam and is broadened by the distribution of velocities. Observing the 431 nm $^3P_1$–$^3P_0$ transition requires prior excitation of the 657 nm clock transition. In that case, excitation of the 657 nm transition is implemented in a spectroscopy region of the vacuum chamber and we apply the blue light further downstream and collect fluorescence. This is illustrated in Fig. 2(c).

B. Characterization of Te_2 Spectrum at 423 nm

The spectrum of tellurium in the vicinity of the 423 nm transition in calcium is shown in Fig. 3. The three plots on the left show the absorption of laser light by tellurium (top), the demodulated MTS signals (middle), and the transverse absorption and longitudinal fluorescence resonances of calcium (bottom). There are three tellurium lines in the ~5 GHz wide spectrum shown. In the right half of the figure, higher resolution curves of a saturated absorption dip and the corresponding MTS signal for the strongest tellurium line are shown.

For saturation of the tellurium resonance at this wavelength, a beam waist of ~1 mm with ~10 mW of power distributed between the pump and probe is required for the MTS setup. For the traces in the figure, the 10 cm Te_2 cell was heated to 400°C. The transition closest to the 423 nm line is relatively strong, and if the cell were heated much higher, the optically thick vapor would prevent the pump and probe beams from interacting with the same molecules and the saturation signal would be lost. On the other hand, the Te_2 signal in the plot that is lower in frequency corresponds to a weaker transition, and this could be easily enhanced by heating the cell further.

As shown in Fig. 3, the closest Te_2 resonance to the calcium 423 nm transition is a strong line about 500 MHz higher in frequency. This line can be used as a frequency reference, but for some purposes a different transition may be preferable. While the weaker Te_2 signal at the lower frequency on the plot is farther from the $^1S_0$–$^1P_1$ resonance, it is closer to the Doppler-shifted frequency for conventional thermal atomic-beam velocities. This Te_2 line may be preferable for frequency locking for laser cooling or for measurements where a reference for fast atoms is desired.

1. Application to Measuring the Instability of the Second-Order Doppler Shift

An example of this latter application is a measurement of the long-term stability of the second-order Doppler shift of a beam clock. The long-term performance of a thermal beam clock is expected to be limited by instabilities in Doppler shifts. Residual first-order Doppler shifts are likely to be a big obstacle to a stable long-term system, but the size and stability of these residual first-order effects are difficult to estimate. Even if first-order shifts could be completely eliminated in a thermal beam, the instability caused by variations in the second-order Doppler shift would still exist and could be a problem; with $\Delta\nu_{(\mathrm{2nd\ Dopp})} = v^2/2c^2 \sim 10^{-12}$ for a thermal calcium beam,

the temperature of the atom source needs to be stable to about 10^{-5} (about 5 mK) to avoid introducing frequency instability above 10^{-17}.

What is achievable in terms of second-order Doppler stability in a thermal beam has not yet been investigated, but as the interest in using these systems as robust clocks grows, a determination of the limits imposed by thermal instabilities would clearly be valuable. The stability floor imposed by variations in the second-order Doppler shift should be at a level that makes it nontrivial to measure directly, especially in the presence of other effects that could be comparable or larger. It should be possible to determine the stability of the atomic beam velocity by looking at the first-order Doppler shift, which can be maximized and made larger than any other effect by sending a laser beam counter-propagating to the atomic beam path. Measuring the stability of the first-order Doppler shift can then be leveraged to determine the stability of the second-order Doppler shift, where the lever arm is c/v, about 5×10^5 for a calcium beam.

Since Doppler shifts are caused by atomic velocity, the fractional frequency fluctuations are the same for all atomic transitions, and for calcium they can be measured with a better signal-to-noise (S/N) ratio using the 423 nm transition than using the 657 nm clock transition. By measuring the frequency difference between the 423 nm Doppler-shifted resonance and the nearest tellurium line, the long-term stability of the beam velocity can be determined. With a width of ~1 GHz, the measurement of the Doppler-shifted resonance with $S/N \sim 100$ should allow measuring the instability of the second-order Doppler shift that integrates as $\sigma \sim 10^{-13}/\tau^{1/2}$, where σ is the Allan deviation characterizing the degree of frequency fluctuations and τ is the averaging time. This could lead to interesting limits at measurement times of days. The tellurium line closest to the Doppler-shifted calcium resonance provides an ideal reference for this proposed measurement, as the proximity in frequency and the long-term stability make it better suited than other alternatives.

C. Tellurium Spectrum at 431 nm

1. Calcium Detection Resonance

In addition to the strong 423 nm transition, calcium has a blue line at 431 nm that is particularly well suited for detection of atoms excited by the 657 nm clock laser. The clock transition couples ground-state $3p^6 4s^2\ {}^1S_0$ atoms to the $3p^6 4s4p\ {}^3P_1$ state, which has a long lifetime of the order of 1 ms. For the fast atomic velocities in a thermal beam, most atoms in this excited sate will never emit a photon in the chamber, let alone scatter multiple photons. On average, the detection of the clock transition by collecting 657 nm photons results in a signal from less than 1 photon per atom.

The $3\ p^6 4p^2\ {}^3P_0$ state that lies 431 nm away from the excited clock state has a short lifetime of tens of nanoseconds (with a corresponding natural width of the order of 30 MHz) before decaying back to $3p^6 4s4p\ {}^3P_1$. Because of angular momentum selection rules, this state can only decay back to the ${}^3P_1$ state via electric dipole coupling. This ${}^3P_0$–${}^3P_1$ transition therefore constitutes a cycling transition that can scatter many blue photons for every atom excited by the 657 nm interrogation laser. Furthermore, it only couples to atoms excited by the 657 nm light; the detection signal from this transition is free from the background of the majority of atoms in the beam that are not excited by the clock laser. Of course, it is not free from laser-light background; the design of collection optics to image the atoms in the path of the 431 nm beam and to block light coming from other locations helps to minimize the stray laser light collected.

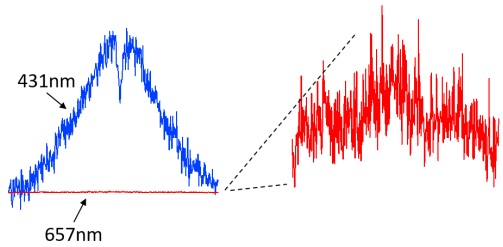

Fig. 4. Left: comparison of atomic resonance curves obtained by detecting emission at 657 nm (red) and laser-induced fluorescence at 431 nm (blue) on the same scale. Right: re-scaled 657 nm signal. Each trace was acquired with a single 50 ms scan of the 657 nm laser frequency and using similar parameters for the photomultiplier tubes. The difference in signal-to-noise ratio between the two methods is about a factor of 10.

The advantage of using the 431 nm transition for detection is illustrated in Fig. 4, which shows two calcium resonances obtained with the two different detection methods. The curves correspond to single sweeps of the clock laser frequency over the entire Doppler profile and were acquired in 50 ms through a 10 kHz low-pass filter, with no additional averaging. The resonances on the left are shown on the same scale and are labeled by which photons are collected; the 657 nm signal is rescaled in the trace on the right.

The data were recorded simultaneously using similar parameters (photomultiplier tubes with similar sensitivities; optical bandpass filters with similar insertion loss at the corresponding wavelength). The improvement of a factor of ~10 in the signal-to-noise ratio from using the 431 nm transition is clearly visible, and further optimization of the blue detection signal should be possible.

2. Tellurium Resonances

The distribution of tellurium resonances in the vicinity of the 431 nm calcium transition is not as favorable as in the 423 nm case, with the closest line being more than 1 GHz away. This makes calibrating the frequency differences between the calcium and tellurium resonances using the modest frequency bandwidth of an acousto-optic modulator challenging; instead, we used a Fizeau-interferometer-based wavelength meter to measure the different resonances with uncertainties of the order of 100 MHz.

The measured wavelength of the ${}^3P_0$–${}^3P_1$ calcium resonance is 430.8951 nm. This resonance and the nearest Te_2 lines are shown in Fig. 5 (recall the setup used to make this measurement in Fig. 2), with more than 10 GHz of the nearby spectrum displayed. A Te_2 line is located at a frequency that is about 1.3 GHz higher than the calcium transition, at a wavelength of 430.8943 nm. This is a somewhat weak transition, requiring a

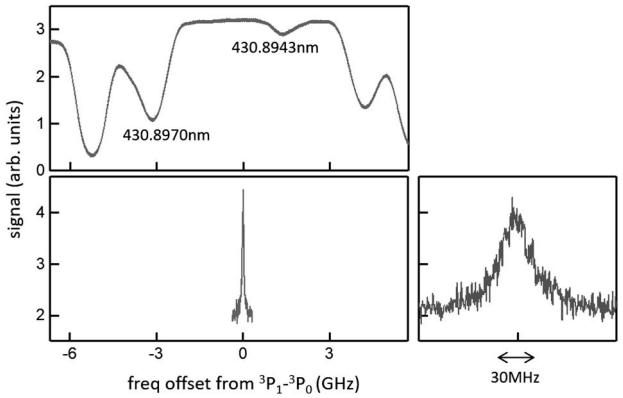

Fig. 5. Tellurium spectrum in the vicinity of $\lambda = 430.8951$ nm. The calcium $^3P_0 - {}^3P_1$ detection resonance (bottom–atomic response as a blue laser is scanned, with a 657 nm laser on resonance) and the nearest tellurium absorption signals (top). The tellurium vapor cell was heated to 470°C for these data. A higher resolution scan of the calcium resonance is shown on the right.

vapor-cell temperature of above 550°C to achieve significant optical depth. A stronger Te_2 transition is located at a wavelength of 430.8970 nm, a full 3 GHz below the calcium detection line. In this case, strong absorption of the pump/probe beams occurs at as low as 400°C.

The frequency separations between these tellurium lines and the calcium resonance are not very convenient. Additionally, saturation intensities for the tellurium resonances at this wavelength are higher than those at 423 nm, requiring power of the order of 30 mW distributed between the pump and probe in order to produce a saturation dip for the strong transition at 430.8970 nm; even with 100 mW of power, no saturation was observable in the weaker 430.8943 nm transition. Locking to the strong resonance using a frequency sideband generated using a high-frequency (∼3 GHz) electro-optic modulator would provide a stabilized laser for the calcium detection resonance.

3. SUMMARY

In conclusion, we have investigated using a tellurium vapor cell as a frequency reference for short-wavelength transitions in neutral calcium. A molecular transition measured in a vapor cell provides a long-term stable frequency reference and can be made compact and robust, to the point of being compatible with operation during transit. This is in contrast to most other frequency stabilization methods such as optical cavities, which exhibit long-term drift and sensitivity to vibrations. Tellurium offers a particularly convenient reference line for fast calcium atoms in a thermal beam. Disadvantages include the amount of optical power required to saturate the tellurium transition, and, for systems where total electrical power is a concern, heating a cell to 500°C could be an obstacle. The required optical power is much less if a simple absorption signal can be used for frequency stabilization. Finally, we point out that a tellurium vapor cell should be useful for a frequency reference or laser stabilization for the $^1S_0$–$^1P_1$ transitions in strontium at 461 nm and ytterbium at 399 nm, as well as for the magic wavelength for a magnesium optical lattice at 468 nm [27].

Acknowledgment. The benefits of using the 431 nm transition in calcium for detection were pointed out to us by Chris Oates, and we benefited from discussions with others working on the calcium optical frequency reference at NIST, especially Judith Olson and Richard Fox. Clock Development at USNO receives funding from the Office of Naval Research.

REFERENCES

1. A. D. Ludlow, M. M. Boyd, J. Ye, E. Peik, and P. O. Schmidt, "Optical atomic clocks," Rev. Mod. Phys. **87**, 637–701 (2015).
2. K. Beloy, N. Hinkley, N. B. Phillips, J. A. Sherman, M. Schioppo, J. Lehman, A. Feldman, L. M. Hanssen, C. W. Oates, and A. D. Ludlow, "Atomic clock with 1×10^{-18} room-temperature blackbody stark uncertainty," Phys. Rev. Lett. **113**, 260801 (2014).
3. B. J. Bloom, T. L. Nicholson, J. R. Williams, S. L. Campbell, M. Bishof, X. Zhang, W. Zhang, S. L. Bromley, and J. Ye, "An optical lattice clock with accuracy and stability at the 10^{-18} level," Nature **506**, 71–75 (2014).
4. N. Huntemann, C. Sanner, B. Lipphardt, C. Tamm, and E. Peik, "Single-ion atomic clock with 3×10^{-18} systematic uncertainty," Phys. Rev. Lett. **116**, 063001 (2016).
5. For a discussion on timekeeping with state-of-the-art operational clocks, refer to the following: S. Peil, T. B. Swanson, J. Hanssen, and J. Taylor, "Microwave-clock timescale with instability on order of 10^{-17}," Metrologia **54**, 247–252 (2017).
6. For an example of integrating a non-continuously running optical clock for timekeeping, refer to the following: C. Grebing, A. Al-Masoudi, S. Dörscher, S. Häfner, V. Gerginov, S. Weyers, B. Lipphardt, F. Riehle, U. Sterr, and C. Lisdat, "Realization of a timescale with an accurate optical lattice clock," Optica **3**, 563–569 (2016).
7. C. Salomon, L. Cacciapuoti, and N. Dimarcq, "Atomic clock ensemble in space: an update," Int. J. Mod. Phys. D **16**, 2511–2523 (2007).
8. J. Grotti, S. Koller, S. Vogt, S. Häfner, U. Sterr, C. Lisdat, H. Denker, C. Voigt, L. Timmen, A. Rolland, F. N. Baynes, H. S. Margolis, M. Zampaolo, P. Thoumany, M. Pizzocaro, B. Rauf, F. Bregolin, A. Tampellini, P. Barbieri, M. Zucco, G. A. Costanzo, C. Clivati, F. Levi, and D. Calonico, "Geodesy and metrology with a transportable optical clock," arXiv:1705.04089 (2017).
9. S. B. Koller, J. Grotti, S. Vogt, A. Al-Masoudi, S. Dörscher, S. Häfner, U. Sterr, and C. Lisdat, "Transportable optical lattice clock with 7×10^{-17} uncertainty," Phys. Rev. Lett. **118**, 073601 (2017).
10. S. Origlia, S. Schiller, M. S. Pramod, L. Smith, Y. Singh, W. He, S. Viswam, D. Świerad, J. Hughes, K. Bongs, U. Sterr, C. Lisdat, S. Vogt, S. Bize, J. Lodewyck, R. Le Targat, D. Holleville, B. Venon, P. Gill, G. Barwood, I. R. Hill, Y. Ovchinnikov, A. Kulosa, W. Ertmer, E.-M. Rasel, J. Stuhler, and W. Kaenders, "Development of a strontium optical lattice clock for the SOC mission on the ISS," Proc. SPIE **9900**, 990003 (2016).
11. X. Zhang, S. Zhang, Z. Jiang, M. Li, H. Shang, F. Meng, W. Zhuang, A. Wang, and J. Chen, "A transportable calcium atomic beam optical clock," in *IEEE International Frequency Control Symposium (IFCS)* (2016).
12. J. J. McFerran and A. N. Luiten, "Fractional frequency instability in the 10^{-14} range with a thermal beam optical frequency reference," J. Opt. Soc. Am. B **27**, 277–285 (2010).
13. R. W. Fox, J. A. Sherman, W. Douglas, J. B. Olson, and C. W. Oates, "A high stability optical frequency reference based on thermal calcium atoms," in *IEEE International Frequency Control Symposium (FCS)* (2012), pp. 404–406.
14. R. L. Barger, J. C. Bergquist, T. C. English, and D. J. Glaze, "Resolution of photon-recoil structure of the 6573-Å calcium line in an atomic beam with optical Ramsey fringes," Appl. Phys. Lett. **34**, 850–852 (1979).
15. A. Morinaga, F. Riehle, J. Ishikawa, and J. Helmcke, "A Ca optical frequency standard: frequency stabilization by means of nonlinear Ramsey resonances," Appl. Phys. B **48**, 165–171 (1989).
16. C. Degenhardt, H. Stoehr, C. Lisdat, G. Wilpers, H. Schnatz, B. Lipphardt, T. Nazarova, P.-E. Pottie, U. Sterr, J. Helmcke, and F. Riehle, "Calcium optical frequency standard with ultracold atoms: approaching 10^{-15} relative uncertainty," Phys. Rev. A **72**, 062111 (2005).

17. G. Wilpers, C. W. Oates, and L. Hollberg, "Improved uncertainty budget for optical frequency measurements with microkelvin neutral atoms: results for a high-stability ^{40}Ca optical frequency standard," Appl. Phys. B **85**, 31–44 (2006).
18. A. J. Murray, M. J. Hussey, and M. Needham, "Design and characterization of an atomic beam source with narrow angular divergence for alkali-Earth targets," Meas. Sci. Technol. **17**, 3094–3101 (2006).
19. C. J. Erickson, B. Neyenhuis, and D. S. Durfee, "High-temperature calcium vapor cell for spectroscopy on the $4s^2\,{}^1S_0$–$4s4p\,{}^3P_1$ intercombination line," Rev. Sci. Instrum. **76**, 123110 (2005).
20. U. Dammalapati, I. Norris, and E. Riis, "Saturated absorption spectroscopy of calcium in a hollow-cathode lamp," J. Phys. B **42**, 165001 (2009).
21. J. McClelland, private communication.
22. I. S. Burns, J. Hult, and C. F. Kaminski, "Use of $^{130}Te_2$ for frequency referencing and active stabilization of a violet extended cavity diode laser," Spectrochim. Acta A **63**, 905–909 (2006).
23. T. J. Scholl, S. J. Rehse, R. A. Holt, and S. D. Rosner, "Absolute wave-number measurements in $^{130}Te_2$: reference lines spanning the 420.9–464.6 nm region," J. Opt. Soc. Am. B **22**, 1128–1133 (2005).
24. L. S. Ma, P. Courteille, G. Ritter, W. Neuhauser, and R. Blatt, "Spectroscopy of Te_2 with modulation transfer: reference lines for precision spectroscopy in Yb^+ at 467 nm," Appl. Phys. B **57**, 159–162 (1993).
25. T. Dutta, D. De Munshi, and M. Mukherjee, "Absolute Te_2 reference for barium ion at 455.4 nm," J. Opt. Soc. Am. B **33**, 1177–1181 (2016).
26. P. Wongwaitayakornkul and T. Killian (unpublished).
27. A. P. Kulosa, D. Fim, K. H. Zipfel, S. Rühmann, S. Sauer, N. Jha, K. Gibble, W. Ertmer, E. M. Rasel, M. S. Safronova, U. I. Safronova, and S. G. Porsev, "Towards a Mg lattice clock: observation of the $^1S_0$–$^3P_0$ transition and determination of the magic wavelength," Phys. Rev. Lett. **115**, 240801 (2015).